Dalton Transactions

COMMUNICATION

View Article Online
View Journal | View Issue

Cite this: *Dalton Trans.*, 2016, **45**, 3272

Received 24th August 2015,
Accepted 25th January 2016

DOI: 10.1039/c6dt00327c

www.rsc.org/dalton

A ruthenium water oxidation catalyst based on a carboxamide ligand†

Wangchuk Rabten,[a] Torbjörn Åkermark,[a] Markus D. Kärkäs,*[a] Hong Chen,[b,c] Junliang Sun,[b,d] Pher G. Andersson*[a] and Björn Åkermark*[a]

Herein is presented a single-site Ru complex bearing a carboxamide-based ligand that efficiently manages to carry out the four-electron oxidation of H_2O. The incorporation of the negatively charged ligand framework significantly lowered the redox potentials of the Ru complex, allowing H_2O oxidation to be driven by the mild oxidant $[Ru(bpy)_3]^{3+}$. This work highlights that the inclusion of amide moieties into metal complexes thus offers access to highly active H_2O oxidation catalysts.

In efforts towards developing a sustainable and clean energy resource, extensive research has been devoted towards splitting of H_2O into O_2 and H_2 (eqn (1)).[1] Here, the design of robust artificial water oxidation catalysts (WOCs) appears to be the stumbling block in attempts to develop systems for the generation of solar fuels. Several research groups are therefore pursuing the construction of robust artificial WOCs based on Ru,[2,3] Mn,[4] Fe,[5] Cu[6] and Co.[7]

$$2H_2O \rightarrow 4H^+ + 4e^- + O_2 \quad (1)$$

In order to develop more efficient WOCs, single-site Ru complexes where the metal is coordinated to a negatively charged ligand have been studied. The use of such ligand frameworks offers the possibility of stabilizing the metal center at a highly oxidized state by electron-donation to the metal center, which results in lowering of the redox potentials.[8] The resulting high-valent metal species are important catalytic intermediates during the oxidation of H_2O and may be key to accessing highly active and robust WOCs.[9] Recent studies focusing on the incorporation of negatively charged ligands have shown that such complexes can result in Ru WOCs with sufficiently low redox potentials to allow H_2O oxidation to be driven by light.[10]

We have recently reported on the unexpected formation of the single-site Ru complex **2** bearing a mixed pyridinecarboxylate ligand (**1**) (Fig. 1). Complex **2** was found to have a sufficiently low redox potential to allow H_2O oxidation to be

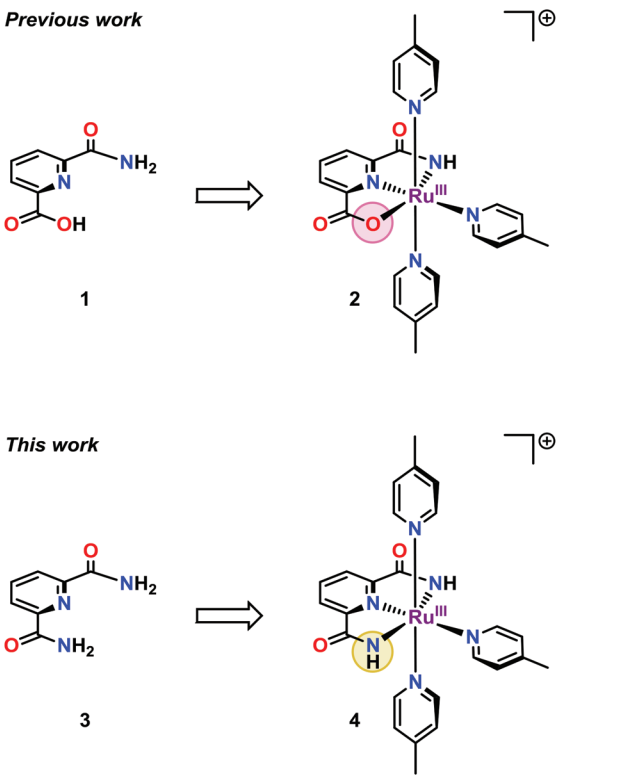

Fig. 1 Structures of the previously reported single-site Ru complex **2** containing ligand **1** and Ru complex **4** based on the dicarboxamide ligand 2,6-pyridine-dicarboxamide (**3**, H_4pdca).

[a]*Department of Organic Chemistry, Arrhenius Laboratory, Stockholm University, SE-106 91 Stockholm, Sweden. E-mail: markus.karkas@su.se, pher.andersson@su.se, bjorn.akermark@su.se*
[b]*Berzelii Centre EXSELENT on Porous Materials, Department of Materials and Environmental Chemistry, Stockholm University, SE-10691 Stockholm, Sweden*
[c]*Faculty of Material Science and Chemistry, China University of Geosciences, 430074 Wuhan, China*
[d]*College of Chemistry and Molecular Engineering, Peking University, 100871 Beijing, China*

† Electronic supplementary information (ESI) available: Experimental details and spectral data. CCDC 1420348. For ESI and crystallographic data in CIF or other electronic format see DOI: 10.1039/c6dt00327c

driven by the mild single-electron oxidant $[Ru(bpy)_3]^{3+}$ (bpy = 2,2′-bipyridine).[11] It was also markedly more active than the corresponding dicarboxylate complex.[12] The incorporation of the amide moiety into WOCs thus seemed to create a suitable ligand framework for producing robust catalysts. It was therefore reasoned that replacing the carboxylate unit in ligand **1** by an additional amide moiety, to give the dicarboxamide ligand **3**, could potentially offer access to an even more active catalyst. Indeed, the substitution of ligand **1** with the dicarboxamide ligand **3** (H_4pdca = 2,6-pyridine-dicarboxamide), resulted in a more active Ru-based WOC (**4**, Fig. 1). When using the mild one-electron oxidant $[Ru(bpy)_3]^{3+}$ at neutral pH, the designed Ru complex **4** managed to reach turnover numbers (TONs) close to 400 and turnover frequencies (TOFs) of ~1.6 s^{-1}, which is almost a two-fold increase compared to Ru complex **2** housing the mixed carboxylate–amide ligand **1**.

Ru complex **4**, $[Ru(H_2pdca)(pic)_3]^+$, was synthesized from the commercially available dicarboxamide ligand **3** (H_4pdca = 2,6-pyridine-dicarboxamide) by refluxing a solution of ligand **3**, $Ru(DMSO)Cl_2$ and Et_3N overnight. To this solution was added 4-picoline and the resulting solution was further refluxed for 48 h. This afforded Ru complex **4** as an orange solid in 25% yield. Complex **4** was characterized by ^{1}H NMR, high-resolution mass spectrometry (HRMS), X-ray crystallography, elemental analysis and UV-vis spectroscopy to confirm the structure of the single-site Ru complex **4**.

Single crystals of X-ray diffraction quality were obtained from an aqueous-methanolic solution. The crystal structure of Ru complex **4** is depicted in Fig. 2. The structure reveals that the Ru^{III} center is located in a slightly distorted $[RuN_6]$ octahedral configuration. The electron-rich dicarboxamide ligand scaffold **3** thus stabilizes the Ru center and makes it possible to isolate the complex at the Ru^{III} state. In the equatorial plane, three positions are occupied by the three nitrogen atoms from the tridentate 2,6-pyridine-dicarboxamide ligand **3**. The fourth position in the equatorial plane and the two axial positions are occupied by 4-picoline ligands.

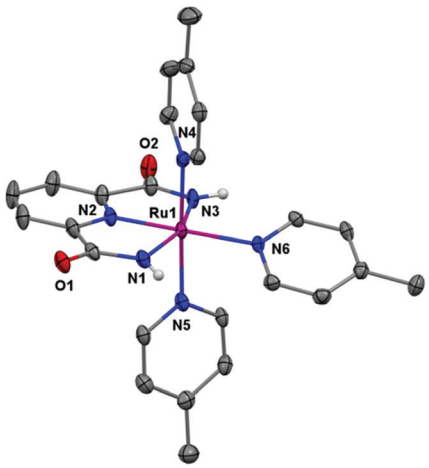

Fig. 2 X-ray crystal structure of the single-site Ru complex **4** at the 50% probability level. Hydrogen atoms (except the N–H) and PF_6 have been omitted for clarity.

Table 1 Selected bond lengths (Å) and angles (°) for Ru complex **4**

Bond lengths			
Ru(1)–N(1)	2.032(2)	Ru(1)–N(4)	2.110(2)
Ru(1)–N(2)	1.973(2)	Ru(1)–N(5)	2.098(2)
Ru(1)–N(3)	2.033(2)	Ru(1)–N(6)	2.117(2)
Bond angles			
N(1)–Ru(1)–N(2)	79.50(8)	N(2)–Ru(1)–N(6)	178.27(7)
N(1)–Ru(1)–N(3)	158.98(7)	N(3)–Ru(1)–N(4)	93.30(7)
N(1)–Ru(1)–N(4)	88.20(7)	N(3)–Ru(1)–N(5)	88.10(7)
N(1)–Ru(1)–N(5)	91.18(7)	N(3)–Ru(1)–N(6)	98.76(7)
N(1)–Ru(1)–N(6)	102.18(7)	N(4)–Ru(1)–N(5)	177.64(7)
N(2)–Ru(1)–N(3)	79.55(8)	N(4)–Ru(1)–N(6)	90.96(7)
N(2)–Ru(1)–N(4)	89.48(7)	N(5)–Ru(1)–N(6)	86.95(7)
N(2)–Ru(1)–N(5)	92.64(7)		

A comparison of the crystal structure of the previously reported Ru^{III} complex **2**,[11] shows that the bond angle N(1)–Ru(1)–N(3) in Ru complex **4** is close to that found in complex **2**, 158.98° and 160.0°, respectively (see Tables 1, S2 and S3†). The Ru–N(pic) distances are all ~2.10 Å, which is longer than in the related Ru^{II} dicarboxylate complex $[Ru(pdc)(pic)_3]^{2+}$ (H_2pdc = 2,6-pyridinedicarboxylic acid).[12] All the Ru–N bond distances are in general slightly longer in Ru complex **4** than those found for complex **2** (see Table S3†).

HRMS analysis of Ru complex **4** in aqueous methanol/acetonitrile solutions showed a major peak at *m*/*z* 544.1172 with a distinct isotopic pattern (Fig. S3†), which can be assigned to $[Ru^{III}(H_2pdca)(pic)_3]^+$ (**4**). Additionally, a peak at *m*/*z* 492.0854 could be observed (Fig. S5†), which corresponds to the acetonitrile-containing Ru-species $[Ru^{III}(H_2pdca)(pic)_2(MeCN)]^+$. In this species, one of the picoline ligands has been displaced for a solvent acetonitrile molecule. However, for the Ru complex to become catalytically active it is important to have access to the corresponding aqua complex. Formation of this aqua complex allows for proton-coupled electron transfer (PCET) and for the synchronous removal of protons and electrons, thus avoiding charge accumulation and high-energy intermediates.[13] The picoline-aqua ligand displacement was therefore studied by HRMS. Upon dissolution of Ru complex **4** in aqueous solutions, a peak at *m*/*z* 469.0683 appeared (Fig. S4†). This peak corresponds to the Ru^{III}-aqua species $[Ru^{III}(H_2pdca)(pic)_2(OH_2)]^+$, which shows that ligand displacement occurs in aqueous solutions to generate the catalytically important Ru-aqua species.

The electrochemical properties of Ru complex **4** were subsequently studied in aqueous solution at neutral pH by cyclic voltammetry (CV) and differential pulse voltammetry (DPV). Under neutral pH, the cyclic voltammogram of complex **4** shows a rapid increase of current at 1.21 V *vs.* NHE, which is due to the catalytic oxidation of H_2O (Fig. S7†). The electrochemistry of Ru complex **4** was further analyzed by DPV under neutral conditions (Fig. S8†). DPV of complex **4** revealed three redox peaks at 0.18, 0.94 and 1.15 V *vs.* NHE (see Table 2). Based on previous work with Ru complex **2**, these events can be assigned to the Ru^{III}/Ru^{II}, Ru^{IV}/Ru^{III} and Ru^{V}/Ru^{IV} redox

Table 2 Summary of the electrochemical data for single-site Ru complex **4** [a]

Redox couple	$E_{1/2}$ (*V vs.* NHE)
Ru^{III}/Ru^{II}	0.18
Ru^{IV}/Ru^{III}	0.94
Ru^{V}/Ru^{IV}	1.15
E_{onset}	1.21

[a] Electrochemical measurements were performed in an aqueous phosphate buffer solution (0.1 M, pH 7.2). All potentials were obtained from DPV and are reported *vs.* NHE. Conditions: scan rate 0.1 V s^{-1}, glassy carbon disk as the working electrode, a platinum spiral as the counter electrode and a saturated calomel electrode (SCE) as the reference electrode. Potentials were converted to NHE by using the $[Ru(bpy)_3]^{3+}/[Ru(bpy)_3]^{2+}$ couple as a standard ($E_{1/2}$ = 1.26 V *vs.* NHE).

couples, respectively. It should be noted that the corresponding redox potentials for the related Ru complex **2** were found to occur at 0.35, 0.72 and 0.92 V *vs*. NHE. From the obtained electrochemical data it is obvious that the substitution of the carboxylate moiety in Ru complex **2** for an amide unit to form Ru complex **4** alters the electrochemical properties of the Ru complex. However, the change is not straightforward because the Ru^{III}/Ru^{II} redox couple is decreased as might be expected, while the higher potentials are increased.

The low onset potential of 1.21 V *vs*. NHE of Ru complex **4** suggests that the complex is able to mediate catalytic H_2O oxidation when driven by the mild single-electron oxidant $[Ru(bpy)_3]^{3+}$. To evaluate Ru complex **4** as a molecular WOC, an aqueous solution (phosphate buffer; 0.1 M, pH 7.2) containing complex **4** was added to the chemical oxidant $[Ru(bpy)_3]^{3+}$. The gaseous products were subsequently analyzed in real-time by mass spectrometry. Indeed, O_2 evolution was immediately triggered upon the addition of an aqueous solution containing Ru complex **4** to the oxidant (Fig. 3). The O_2 evolution dependence on pH was also investigated and it could be shown that pH 6.0 and 7.2 afforded the highest catalytic activity (see Fig. S13 and Table S1†). Background experiments were also carried out to verify that complex **4** is necessary for maintaining catalytic activity. In the absence of Ru complex **4**, spontaneous decomposition of the $[Ru(bpy)_3]^{3+}$ oxidant occurs without any detectable formation of O_2, highlighting that complex **4** is essential for oxidizing H_2O. It should be noted that the low O_2 evolution yields, *i.e.* conversion yields from oxidant to O_2, depicted in Table 3 are due to competing pathways in which the chemical oxidant $[Ru(bpy)_3]^{3+}$ is spontaneously decomposed, thus resulting in unproductive reaction pathways without any evolution of O_2.

The catalytic activity of Ru complex **4** was compared with that of the previously developed $[Ru(bpb)(pic)_2]^{+}$ complex (H_2bpb = *N*,*N*′-1,2-phenylene-bis(2-pyridine-carboxamide)), based on a tetradentate bisamide ligand scaffold, where O_2 evolution halted after ~200 TONs because of the formation of the catalytically inactive mono-carbonyl complex $[Ru(bpb)(CO)(OH_2)]$.[8c] By contrast, such species do not appear to interfere with Ru complexes **2** and **4**. It is also important to compare

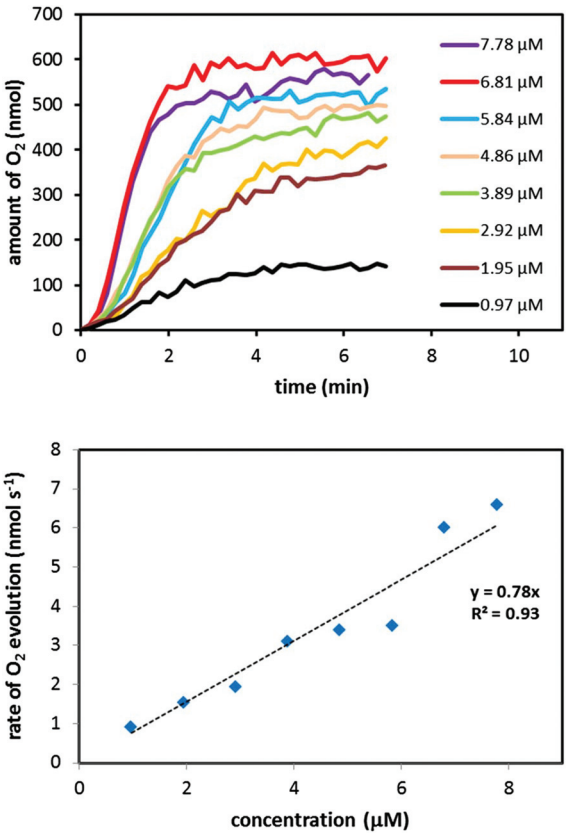

Fig. 3 (upper) Plots of O_2 evolution *versus* time at various concentrations of Ru complex **4**. Reaction conditions: an aqueous phosphate buffer solution (0.1 M, pH 7.2, 0.50 mL) containing Ru complex **4** was added to the oxidant $[Ru(bpy)_3](PF_6)_3$ (3.6 mg, 3.6 μmol). (lower) Initial rate of O_2 evolution plotted as a function of the concentration of Ru complex **4**. Rates of O_2 evolution were calculated from the slopes of linearly fitted O_2 evolution plots in the period of 30–90 s.

Table 3 Summary of the catalytic data for Ru complex **4** [a]

Catalyst concentration (μM)	TON[b] (nmol O_2/nmol cat.)	Yield of O_2 (4·amount O_2/amount oxidant)
7.78	149	64.4%
6.81	181	68.5%
5.84	183	59.4%
4.86	214	57.9%
3.89	269	58.2%
2.92	305	49.4%
1.95	388	41.9%
0.97	319	17.2%

[a] Reaction conditions: an aqueous phosphate buffer solution (0.1 M, pH 7.2, 0.50 mL) containing Ru complex **4** was added to the oxidant $[Ru(bpy)_3](PF_6)_3$ (3.6 mg, 3.6 μmol). [b] Turnover numbers (TONs) were calculated from moles of produced O_2/moles of catalyst.

the catalytic efficiencies of Ru complexes **2** and **4**. Ru complex **4** is able to generate a TON of ~400 and a TOF of ~1.6 s^{-1}, while complex **2**[11] is less efficient and produces a TON of ~200 and a TOF of ~1.32 s^{-1}. Although Ru complexes **2** and **4** have a

high structural resemblance and share almost the same tridentate ligand framework, there is a difference in catalytic activity. This effect is not clear but could originate from the labile carboxylate unit that exists in the ligand scaffold in Ru complex **2**. It has previously been found that high-valent Ru-oxo species are prone to undergo extrusion of CO_2 with subsequent cleavage of the (hetero)aryl–carbonyl bond.[14] This sort of Ru-catalyzed decarboxylation would hence be regarded as an unfavorable reaction pathway that limits the catalytic activity of Ru complex **2**. The small structural change when changing the carboxylate unit in complex **2** to an amide moiety in complex **4** apparently has a significant impact on the catalytic activity. Realizing these small, but fundamental, structural variations in artificial WOCs could thus be of value for the development of more robust WOCs.

To conclude, through a rational molecular design, a highly active WOC has been developed based on a carboxamide ligand scaffold. The designed Ru complex **4** was found to have a low overpotential for H_2O oxidation, which is attractive, and thus enabled H_2O oxidation to be driven by the mild chemical oxidant $[Ru(bpy)_3]^{3+}$. It could be established that when driven by $[Ru(bpy)_3]^{3+}$, Ru complex **4** generated a TON close to 400, which is almost a two-fold increase compared to Ru complex **2** that is based on the mixed carboxylate–amide ligand **1**. These findings are intriguing and it is believed that the results presented herein will contribute to further development of Ru-based WOCs for creating sustainable H_2O splitting devices.

Acknowledgements

Financial support from the Swedish Research Council (621-2013-4872 and 348-2014-6070), the Knut and Alice Wallenberg Foundation and the Carl Trygger Foundation is gratefully acknowledged. We would also like to thank Beamline I19 at Diamond Light Source, UK for crystal data collection.

Notes and references

1 (*a*) M. D. Kärkäs, E. V. Johnston, O. Verho and B. Åkermark, *Acc. Chem. Res.*, 2014, **47**, 100; (*b*) W. Lubitz, E. J. Reijerse and J. Messinger, *Energy Environ. Sci.*, 2008, **1**, 15.

2 For recent examples of single-site ruthenium-based water oxidation catalysts, see: (*a*) M. R. Norris, J. J. Concepcion, Z. Fang, J. L. Templeton and T. J. Meyer, *Angew. Chem., Int. Ed.*, 2013, **52**, 13580; (*b*) C. J. Richmond, R. Matheu, A. Poater, L. Falivene, J. Benet-Buchholz, X. Sala, L. Cavallo and A. Llobet, *Chem. – Eur. J.*, 2014, **20**, 17282; (*c*) L. Wang, L. Duan, Y. Wang, M. S. G. Ahlquist and L. Sun, *Chem. Commun.*, 2014, **50**, 12947; (*d*) T.-T. Li, W.-L. Zhao, Y. Chen, F.-M. Li, C.-J. Wang, Y.-H. Tian and W.-F. Fu, *Chem. – Eur. J.*, 2014, **20**, 13957; (*e*) Y. Liu, S.-M. Ng, S.-M. Yiu, W. W. Y. Lam, X.-G. Wei, K.-C. Lau and T.-C. Lau, *Angew. Chem., Int. Ed.*, 2014, **53**, 14468; (*f*) J. T. Muckerman, M. Kowalczyk, Y. M. Badiei, D. E. Polyansky, J. J. Concepcion, R. Zong, R. P. Thummel and E. Fujita, *Inorg. Chem.*, 2014, **53**, 6904; (*g*) Y. Wang and M. S. G. Ahlquist, *Phys. Chem. Chem. Phys.*, 2014, **16**, 11182; M. D. Kärkäs, R.-Z. Liao, T. M. Laine, T. Åkermark, S. Ghanem, P. E. M. Siegbahn and B. Åkermark, *Catal. Sci. Technol.*, 2016, DOI: 10.1039/C5CY01704A; (*h*) M. D. Kärkäs, R.-Z. Liao, T. M. Laine, T. Åkermark, S. Ghanem, P. E. M. Siegbahn and B. Åkermark, *Catal. Sci. Technol.*, 2016, DOI: 10.1039/C5CY01704A.

3 For recent examples of dinuclear ruthenium-based water oxidation catalysts, see: (*a*) Y. Xu, A. Fischer, L. Duan, L. Tong, E. Gabrielsson, B. Åkermark and L. Sun, *Angew. Chem., Int. Ed.*, 2010, **49**, 8934; (*b*) S. Neudeck, S. Maji, I. López, S. Meyer, F. Meyer and A. Llobet, *J. Am. Chem. Soc.*, 2014, **136**, 24; (*c*) H. Isobe, K. Tanaka, J.-R. Shen and K. Yamaguchi, *Inorg. Chem.*, 2014, **53**, 3973; (*d*) T. M. Laine, M. D. Kärkäs, R.-Z. Liao, T. Åkermark, B.-L. Lee, E. A. Karlsson, P. E. M. Siegbahn and B. Åkermark, *Chem. Commun.*, 2015, **51**, 1862; (*e*) T. M. Laine, M. D. Kärkäs, R.-Z. Liao, P. E. M. Siegbahn and B. Åkermark, *Chem. – Eur. J.*, 2015, **21**, 10039.

4 For examples of manganese-based water oxidation catalysts, see: (*a*) E. A. Karlsson, B.-L. Lee, T. Åkermark, E. V. Johnston, M. D. Kärkäs, J. Sun, Ö. Hansson, J.-E. Bäckvall and B. Åkermark, *Angew. Chem., Int. Ed.*, 2011, **50**, 11715; (*b*) K. J. Young, B. J. Brennan, R. Tagore and G. W. Brudvig, *Acc. Chem. Res.*, 2015, **48**, 567; (*c*) W. A. A. Arafa, M. D. Kärkäs, B.-L. Lee, T. Åkermark, R.-Z. Liao, H.-M. Berends, J. Messinger, P. E. M. Siegbahn and B. Åkermark, *Phys. Chem. Chem. Phys.*, 2014, **16**, 11950; (*d*) K. Yamamoto, S. Nakazawa and T. Imaoka, *Mol. Cryst. Liq. Cryst.*, 2002, **379**, 407; (*e*) E. A. Karlsson, B.-L. Lee, R.-Z. Liao, T. Åkermark, M. D. Kärkäs, V. Saavedra Becerril, P. E. M. Siegbahn, X. Zou, M. Abrahamsson and B. Åkermark, *ChemPlusChem*, 2014, **79**, 936; (*f*) L. Ma, Q. Wang, W.-L. Man, H.-K. Kwong, C.-C. Ko and T.-C. Lau, *Angew. Chem., Int. Ed.*, 2015, **54**, 5246; (*g*) R.-Z. Liao, M. D. Kärkäs, B.-L. Lee, B. Åkermark and P. E. M. Siegbahn, *Inorg. Chem.*, 2015, **54**, 342.

5 For examples of iron-based water oxidation catalysts, see: (*a*) F. Acuña-Parés, M. Costas, J. M. Luis and J. Lloret-Fillol, *Inorg. Chem.*, 2014, **53**, 5474; (*b*) C. Panda, J. Debgupta, D. Díaz Díaz, K. K. Singh, S. Sen Gupta and B. B. Dhar, *J. Am. Chem. Soc.*, 2014, **136**, 12273; (*c*) R.-Z. Liao, X.-C. Li and P. E. M. Siegbahn, *Eur. J. Inorg. Chem.*, 2014, 728; (*d*) M. K. Coggins, M.-T. Zhang, A. K. Vannucci, C. J. Dares and T. J. Meyer, *J. Am. Chem. Soc.*, 2014, **136**, 5531; (*e*) A. R. Parent, T. Nakazono, S. Lin, S. Utsunomiya and K. Sakai, *Dalton Trans.*, 2014, **43**, 12501.

6 For examples of copper-based water oxidation catalysts, see: (*a*) S. M. Barnett, K. I. Goldberg and J. M. Mayer, *Nat. Chem.*, 2012, **4**, 498; (*b*) D. L. Gerlach, S. Bhagan, A. A. Cruce, D. B. Burks, I. Nieto, H. T. Truong, S. P. Kelley, C. J. Herbst-Gervasoni, K. L. Jernigan, M. K. Bowman,

S. Pan, M. Zeller and E. T. Papish, *Inorg. Chem.*, 2014, **53**, 12689; (*c*) S. G. Winikoff and C. J. Cramer, *Catal. Sci. Technol.*, 2014, **4**, 2484.

7 For examples of cobalt-based water oxidation catalysts, see: (*a*) H.-Y. Wang, E. Mijangos, S. Ott and A. Thapper, *Angew. Chem., Int. Ed.*, 2014, **53**, 14499; (*b*) X. Zhou, F. Li, H. Li, B. Zhang, F. Yu and L. Sun, *ChemSusChem*, 2014, **7**, 2453; (*c*) M. Chen, S.-M. Ng, S.-M. Yiu, K.-C. Lau, R. J. Zeng and T.-C. Lau, *Chem. Commun.*, 2014, **50**, 14956; (*d*) H. Lv, J. Song, Y. V. Geletii, J. W. Vickers, J. M. Sumliner, D. G. Musaev, P. Kögerler, P. F. Zhuk, J. Bacsa, G. Zhu and C. L. Hill, *J. Am. Chem. Soc.*, 2014, **136**, 9268; (*e*) I. Siewert and J. Gałęzowska, *Chem. – Eur. J.*, 2015, **21**, 2780; (*f*) N. Morlanés, K. S. Joya, K. Takanabe and V. Rodionov, *Eur. J. Inorg. Chem.*, 2015, 49; (*g*) B. Das, A. Orthaber, S. Ott and A. Thapper, *Chem. Commun.*, 2015, **51**, 13074.

8 (*a*) M. D. Kärkäs, E. V. Johnston, E. A. Karlsson, B.-L. Lee, T. Åkermark, M. Shariatgorji, L. Ilag, Ö. Hansson, J.-E. Bäckvall and B. Åkermark, *Chem. – Eur. J.*, 2011, **17**, 7953; (*b*) L. Duan, A. Fischer, Y. Xu and L. Sun, *J. Am. Chem. Soc.*, 2009, **131**, 10397; (*c*) M. D. Kärkäs, T. Åkermark, H. Chen, J. Sun and B. Åkermark, *Angew. Chem., Int. Ed.*, 2013, **52**, 4189.

9 M. D. Kärkäs, O. Verho, E. V. Johnston and B. Åkermark, *Chem. Rev.*, 2014, **114**, 11863.

10 (*a*) Y. Xu, L. Duan, L. Tong, B. Åkermark and L. Sun, *Chem. Commun.*, 2010, **46**, 6506; (*b*) M. D. Kärkäs, T. Åkermark, E. V. Johnston, S. R. Karim, T. M. Laine, B.-L. Lee, T. Åkermark, T. Privalov and B. Åkermark, *Angew. Chem., Int. Ed.*, 2012, **51**, 11589.

11 W. Rabten, M. D. Kärkäs, T. Åkermark, H. Chen, R.-Z. Liao, F. Tinnis, J. Sun, P. E. M. Siegbahn, P. G. Andersson and B. Åkermark, *Inorg. Chem.*, 2015, **54**, 4611.

12 L. Duan, Y. Xu, M. Gorlov, L. Tong, S. Andersson and L. Sun, *Chem. – Eur. J.*, 2010, **16**, 4659.

13 C. Costentin, M. Robert and J.-M. Savéant, *Acc. Chem. Res.*, 2010, **43**, 1019.

14 L. J. Gooßen, N. Rodríguez and K. Gooßen, *Angew. Chem., Int. Ed.*, 2008, **47**, 3100.

